

# Enhanced photocatalytic activity of hierarchically micro-/nano-porous TiO<sub>2</sub> films

Yong Zhao<sup>a,c</sup>, Xintong Zhang<sup>b</sup>, Jin Zhai<sup>a,\*</sup>, Jinling He<sup>a,c</sup>, Lei Jiang<sup>a</sup>, Zhaoyue Liu<sup>b</sup>,  
Shunsuke Nishimoto<sup>b</sup>, Taketoshi Murakami<sup>b</sup>, Akira Fujishima<sup>b,\*</sup>, Daoben Zhu<sup>a</sup>

<sup>a</sup> Beijing National Laboratory for Molecular Sciences (BNLMS), Center for Molecular Science, Institute of Chemistry,  
Chinese Academy of Sciences, Beijing 100080, China

<sup>b</sup> Kanagawa Academy of Science and Technology, KSP Building West 614, 3-2-1 Sakado, Takatsu-ku, Kawasaki, Kanagawa 213-0012, Japan

<sup>c</sup> Graduate School of the Chinese Academy of Sciences, Beijing 100080, China

Received 20 November 2007; received in revised form 21 January 2008; accepted 26 January 2008

Available online 12 February 2008

## Abstract

Photocatalytic activity of hierarchically micro-/nano-porous film is studied for the first time. The results show its catalytic activity was increased ca. 30–40% and ca. 60–70% for mineralizing gaseous acetaldehyde and liquid-phase phenol, respectively, comparing to that of nano-structured film. Hierarchical TiO<sub>2</sub> porous film produces continuously composite pore channels, providing the fast transport pathway for reactants, products and O<sub>2</sub> moving into and out of the catalytic framework. Additionally, due to extended optical path length from light scattering effect in composite film, the light-absorption efficiency is enhanced distinctly in the range of 380–410 nm, which is close to P25 TiO<sub>2</sub> band-gap edge. The presented investigation indicates that the pores structure plays important roles in the photocatalytic characters of films photocatalyst. More important, the as-prepared film catalyst gives a promising future for its actual application.

© 2008 Elsevier B.V. All rights reserved.

**Keywords:** TiO<sub>2</sub>; Hierarchical structure; Photocatalytic; Composite channels

## 1. Introduction

Titanium dioxide (TiO<sub>2</sub>), since first report of the Honda–Fujishima effect, has received great attention in a range of scientific and industrial fields, such as light-induced water splitting [1–4], dye-sensitized solar cell [5,6], and self-cleaning surface [7–9]. Due to its unique electronic, optoelectronic, and catalytic properties, photo-degradation of organic contaminant becomes one of the most important applications of TiO<sub>2</sub>, which is a fast growing research area in the recent years [10–15]. In order to increase TiO<sub>2</sub> photocatalytic activity, many methods are put forward, such as selecting TiO<sub>2</sub> nano-crystalline particles [16,17], doped with metal [18,19] and nonmetal elements [20–22], coupling with other semiconductors [23,24], and so on [25,26]. The modification of compositions can reduce

the fast recombination of the photogenerated carriers by increasing charge separation, therefore improving the efficiency of catalytic reaction. Although much progress has been achieved by the above strategies, the non-porous and nano-porous photocatalysts suffered lots of limits: low light-captured efficiency, poor in-film diffusion of molecules or small surface area. And then low catalytic quantum efficiencies were revealed in these systems [27,28]. Therefore, designing a catalytic system with effective utilization of solar energy, quick transfer of molecules and bigger surface area is a crucial point in scientific research and actual application.

The porous structure of micro- or nano-structured system take significant parts in its' physical/chemical character. Whether the final chemistry is labeled as catalysis, sensing, energy storage, synthesis, or fabrication, the reactions are most effective when the transport paths through which molecules move into or out of the porous material are included as an integral part of the architectural design [29]. As a chemical reaction is carried out in porous catalyzers, more active centers will be obtained, and the reactants and products transferred in the porous transport

\* Corresponding authors. Tel.: +86 10 82621396; fax: +86 10 82627566.

E-mail addresses: [zhaijin@iccas.ac.cn](mailto:zhaijin@iccas.ac.cn) (J. Zhai), [fujishima@newkast.or.jp](mailto:fujishima@newkast.or.jp) (A. Fujishima).

channels will become easy [30,31]. Therefore, tailoring textural parameters of the  $\text{TiO}_2$  material, such as pore-size distribution, crystallinity and surface area, can be considered as effective methods to better understand the photocatalytic mechanism and improve photocatalytic properties. Based on the ideas, many interestingly textural materials are synthesized to degrade organic pollutants, such as nanofibers [32,33], nanotubes [34,35], foam [36], spheres [37] or other morphology [38–40], and lots of results are fascinating. But, unfortunately, most of these special porous materials are just the powder or the process of fabrication is complicate, and they cannot meet the current industrial demands. In the design of photochemical reactor and actual application, especially for mineralizing liquid pollutant, immobilized film photocatalysts are more important than those of powder and suspension photocatalysts, because the recovery and reuse is facilitated.

In this paper, a newly hierarchical  $\text{TiO}_2$  porous film was employed to conduct the photocatalytic researches. A series of experiments aimed to investigate the relationship between the porous structure and catalytic performance were described. Liquid phenol and gaseous acetaldehyde were selected as double probes. We compared the catalytic character of micro-/nano-hierarchical films with that of nano-structured films. The results showed that the photocatalytic activity can be enhanced largely by the hierarchical structure, which is due to easier access of molecules to reactive sites, enhanced light-captured efficiency of P25  $\text{TiO}_2$  band-gap edge and higher surface area in the composite porous system. To best of our knowledge, this is the first time to construct the hierarchical micro-/nano-structure in film photocatalysis, and also it can be fabricated on any solid substrate in large area.

## 2. Experimental

### 2.1. Materials and instrumentation

$\text{TiO}_2$  powder (Degussa P25, Nippon Aerisol), polyvinyl alcohol (PVA,  $M_w$  20,000, Wako), phenol (Wako) were used as received without purification. Copper mesh (100 mesh) was purchased from Nilaco Company. Acetaldehyde (1 vol% in  $\text{N}_2$ ) was obtained from Takachiko. Borosilicate glass slides were used as substrates for  $\text{TiO}_2$  films, and were dip-coated with a dense  $\text{SiO}_2$  layer (NDH-500C, Nihon Soda) before the deposition of  $\text{TiO}_2$  in order to block the sodium diffusion from glass to  $\text{TiO}_2$  films. Deionized water (18  $M\Omega$  cm) was used in all the experiments.

Surface morphologies of  $\text{TiO}_2$  films were examined with a Hitachi S-4800 scanning electron microscope (SEM). The crystal morphology of  $\text{TiO}_2$  films was analyzed with a Rigaku RINT1500 diffractometer with graphite-monochromatized  $\text{Cu K}\alpha$  radiation. UV–vis measurements were taken with a Shimadzu UV-2450 spectrophotometer, equipped with an integrated sphere. The Brunauer–Emmett–Teller (BET) surface area of the  $\text{TiO}_2$  film catalysts was measured with a surface area analyzer (Macorb HM Model-1208). The micrographs of copper mesh with  $\text{TiO}_2$  porous films were taken with an optical microscope (Keyence VH-100).

The concentration of phenol was measured with a high-performance liquid chromatography system (HPLC, LC-2010, Shimadzu). The concentration of acetaldehyde and carbon dioxide was traced with a gas chromatography (GC-8A, Shimadzu), equipped with a 2-m Porapak-Q column, and a flame ionization detector, using  $\text{N}_2$  as the carrier gas.

### 2.2. Preparation of $\text{TiO}_2$ film photocatalysts

Micro-/nano-composite hierarchical  $\text{TiO}_2$  films were prepared on glass substrates by electro-hydrodynamic (EHD) method. The experimental details can be found elsewhere [41]. In brief, 0.6 g  $\text{TiO}_2$  was added into a mixture of solution containing PVA aqueous solution (1.2 g, 25 wt%), ethanol (4 mL) and water (4 mL), and was dispersed into stable suspension with a ultrasonic homogenizer (Sonic vibra-cell). The suspension was loaded into a glass syringe, and sprayed onto glass substrates driven by an electric field of  $1.5 \text{ kV cm}^{-1}$ . In a continuous-spraying mode,  $\text{TiO}_2$ -PVA hybrid microspheres were deposited randomly on the surface of glass substrate to form organic/inorganic composite film layer by layer. During the course of  $\text{TiO}_2$ -polymer micro-spheres deposition under the strong electric field, lots of submicro-channels were formed among the interspaces of  $\text{TiO}_2$  microspheres in the film. After calcination in air at 723 K for 1 h,  $\text{TiO}_2$  porous films with hierarchical branched inner channels were prepared. The amount of  $\text{TiO}_2$  nanoparticles on the film is controlled at  $12 \pm 1 \text{ mg}$ .

Nano-structured films were prepared by spin-coating  $\text{TiO}_2$  suspension on  $\text{SiO}_2$ -coated glass substrates at 1000 rpm. The thin films with the definite  $\text{TiO}_2$  weight ( $12 \pm 1 \text{ mg}$ ) were obtained after repeating the above procedure for several times. The thickness of nano-structured films was about  $1.5 \mu\text{m}$ , a bit thinner than the  $2\text{-}\mu\text{m}$ -thick micro-/nano-structured films.

### 2.3. Photocatalytic reaction

Decomposition of phenol: the photo-degradation of phenol in water solution (20 ppm, 50 mL) was carried out in a 100-mL Pyrex glass vessel with magnetic stirring. UV irradiation was supplied by a Hg–Xe lamp (LA-310 UV), which was equipped with a filter to emit UV light in the range of 300–420 nm. Before experiments,  $\text{TiO}_2$  film photocatalysts were pretreated under UV light illumination for 30 min. And then the  $\text{TiO}_2$  films were immersed in the solution and fixed in the middle of the vessel perpendicular to the light beam. After keeping in the dark for 30 min, the film photocatalysts were irradiated with UV light ( $4 \text{ mW cm}^{-2}$ ). The temperature of photocatalytic system was kept at about 298 K during the experiments. The residual concentration of phenol was measured through a HPLC.

Decomposition of acetaldehyde: decomposition of gaseous acetaldehyde was carried out in a 500-mL Pyrex glass reactor vessel covered with a quartz plate at room temperature.  $\text{TiO}_2$  film photocatalysts were put on the bottom of glass vessel, and were irradiation with black-light lamps ( $1.2 \text{ mW cm}^{-2}$ ) through the quartz plate. The vessel was filled with an  $\text{O}_2$

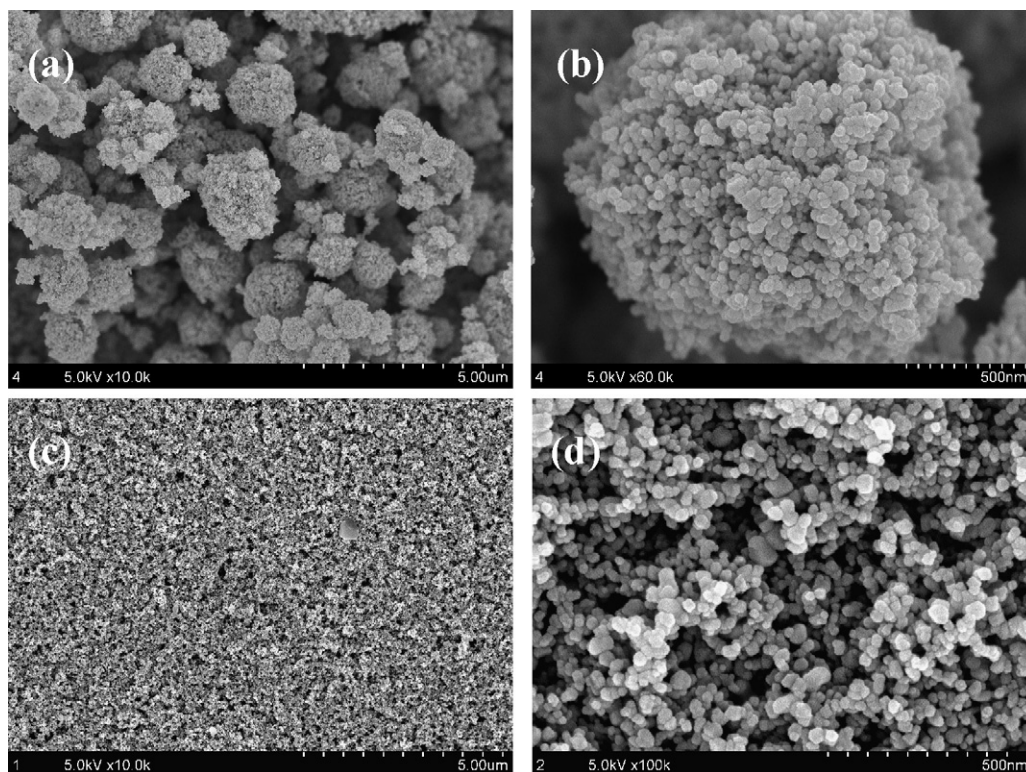


Fig. 1. (a) SEM image of micro-/nano-hierarchically porous film prepared from EHD method. (b) The higher magnification image of (a). (c) SEM image of nano-structured film prepared by spin-coating method. (d) The higher magnification image of (c).

(20%)–N<sub>2</sub> gas mixture adjusted to a relative humidity of 50%. Measured quantities of acetaldehyde (1 vol% in N<sub>2</sub>) were injected into the reactor using a syringe. The system was kept in dark for 2 h, and then was irradiated with UV light. Concentrations of acetaldehyde and carbon dioxide were followed by gas chromatography.

### 3. Results and discussion

#### 3.1. Fabrication and characterization of TiO<sub>2</sub> micro-/nano-hierarchical film

The fabrication process of TiO<sub>2</sub> micro-/nano-composite film was described elsewhere in detail [41]. Fig. 1a and b shows SEM images of a micro-/nano-composite film prepared by the EHD technique. The top surface given in Fig. 1a is composed of lots of TiO<sub>2</sub> micro-scale and sub-micro-scale near-spheres with the diameter of 100 nm to 1 μm. It is also clear from the image that numerous disorderly macropores are obtained among the micro-spheres, and continuous textural macro-porous channels can be found in the film. From the enlarged image in Fig. 1b, it can be seen that the macro-sphere is assembled by TiO<sub>2</sub> nanoparticles, while nanopores among the nanoparticles can be found in the sphere. Macropores and nanopores in the film construct the continuously and hierarchically porous channels. Fig. 1c and d indicates SEM images of nano-structured film prepared by spin-coating method. The surface of TiO<sub>2</sub> nano-films appears to be very smooth and the size of pores is less than 100 nm. The previous research shows the pore distribution of

nano-structured film is centered in the range of mesoporosity [41]. Fig. 2 is an XRD pattern of the TiO<sub>2</sub> micro-/nano-composite film, showing a mixture of anatase and rutile.

#### 3.2. Photo-degradation of gaseous acetaldehyde and liquid-phase phenol

In order to evaluate the photocatalytic activity of TiO<sub>2</sub> micro-/nano-hierarchical films, the photo-decomposition of gaseous acetaldehyde and liquid phenol were introduced to test. Fig. 3 indicated typical experimental data for the decomposi-

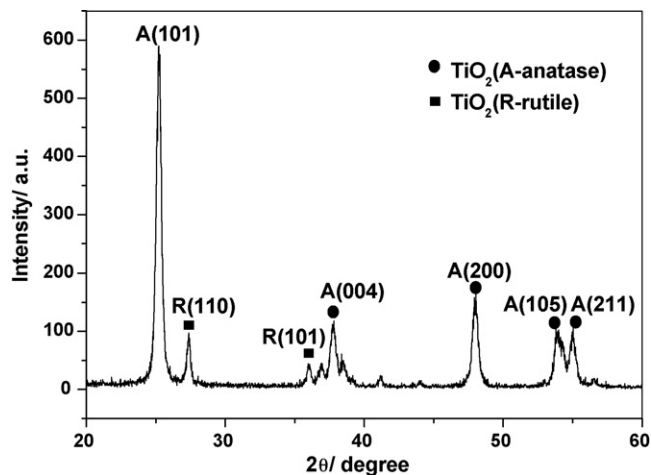


Fig. 2. X-ray diffraction patterns of TiO<sub>2</sub> porous films. It shows a mixture of anatase and rutile.



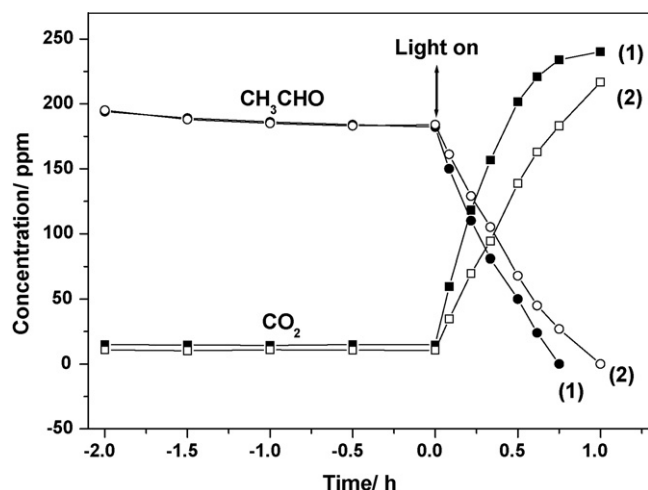


Fig. 3. Photodecomposition of acetaldehyde and production of  $\text{CO}_2$  with (1) (●, ■) micro-/nano-hierarchically porous film and (2) (○, □) nano-structured film as a function of irradiation time with the black light lamp.

tion of acetaldehyde and generated  $\text{CO}_2$  concentrations within the  $\text{TiO}_2$  film as a function of illumination time. At equilibrium, the amount of acetaldehyde in the reaction vessels decreased little under all conditions, which can be explained that acetaldehyde was absorbed physically or chemically by the porous  $\text{TiO}_2$  samples because of no increase for concentration of  $\text{CO}_2$ . Herein, nano-structured films with the same amount of  $\text{TiO}_2$  nanoparticles ( $12 \pm 1$  mg) were selected as reference to investigate the influence of porous structure on the photocatalytic activity. The three-to-four samples were selected to repeat the experiments and the average values were shown here. The rate of mineralizing pollutant was evaluated by the equation  $K = \ln[C_0/C(t)]/t$  [42], where  $C(t)$  is the concentration of reactant,  $C_0$  is initial concentration of reactant,  $t$  is reaction time and  $K$  is pseudo first-order rate constant. According to the equation, the rate constant of decomposing acetaldehyde for hierarchical structured film ( $K_{\text{micro-/nano-film}}$ ) was about  $2.4 \text{ h}^{-1}$ , exhibiting better catalytic activity than that of nano-structured film ( $K_{\text{nano-film}} \approx 1.7 \text{ h}^{-1}$ ). There is 30–40% increase for the rate of decomposing acetaldehyde. Along with the decrease of acetaldehyde, the discrepancy of generated  $\text{CO}_2$  rates also proves the higher activity of hierarchical structure. In Fig. 3, the ratio of production of  $\text{CO}_2$  to removal of acetaldehyde  $r_{\text{CO}_2}/r_{\text{CH}_3\text{CHO}}$  is smaller than 2:1, the part deviated from stoichiometry is the intermediate products, such as acetic acid. Furthermore,  $r_{\text{CO}_2}/r_{\text{CH}_3\text{CHO}}$  for micro-/nano-composite film and nano-film is about 1.4 and 1, respectively. Therefore, it is safe to say hierarchical thin film is better for the complete mineralization of acetaldehyde. Probably, the hierarchical open structure let the diffusion of reactants, products and  $\text{O}_2$  inside film easier than that of the nano-film. In the photocatalytic degradation process, an abundant oxygen supply is important for the mineralization. Mineralization in pure oxygen is much faster than in air, though the removal of target compounds is the same rate in air or in pure oxygen.

In order to obtain more incisive insights into the influence of porous structure on the photocatalytic activity, liquid-phase phenol is also chosen to study. The  $\text{TiO}_2$  samples are the same

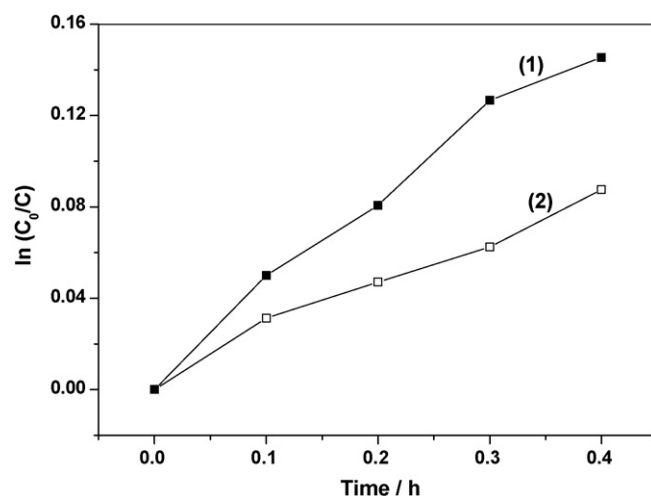


Fig. 4. Photocatalytic degradation of phenol with (1) (■) micro-/nano-hierarchically porous film and (2) (□) nano-structured film.

to those used in decomposing  $\text{CH}_3\text{CHO}$  after regenerating them under UV irradiation. Phenol is hardly adsorbed on catalysts such as  $\text{TiO}_2$  or some other photocatalysts else from its aqueous solution, so its mineralization is always more difficult than the adsorbable pollutants. Selecting phenol as a probe is significant to discuss the effect of textural discrepancy on the photocatalytic activity. Fig. 4 shows the photocatalytic activity of two  $\text{TiO}_2$  films on the degradation of phenol. It can be seen clearly that the activity of the hierarchically porous film is higher than that of nano-films. As discussed in the photo-oxidizing  $\text{CH}_3\text{CHO}$ , photo-degradation result is also estimated by rate constant  $K$ . The linear correlation at initial stage of photocatalytic experiments between  $\ln(C_0/C)$  and  $t$  suggests a first-order reaction for the two types of thin films. The rate constant of decomposing phenol for hierarchical structured film is  $0.36 \text{ h}^{-1}$ , which shows higher activity than nano-structured film,  $0.21 \text{ h}^{-1}$ . There is about 60–70% increase in photocatalytic activity with the composite hierarchical structure in the film.

### 3.3. Mechanisms

The photocatalytic activity, that is, the efficiency of mineralizing pollutant, is determined by light-harvesting efficiency, efficiency of the reaction of photogenerated electron/hole, and the rate of electron/hole recombination [43,44]. Light-collection efficiency is strongly influenced by the morphology structure of photocatalyst. In the hierarchical structured  $\text{TiO}_2$  film, continuous macrochannels can be acted as big light-transferred way to let the incident photon flux into the inner surface of mesoporous  $\text{TiO}_2$  and extend optical paths length, obtaining more efficient light-collection case. Fig. 5 exhibits the UV–vis absorption spectra of the  $\text{TiO}_2$  micro-/nano-composite film and nano-structured film. It can be seen clearly that light absorption at the wavelength from 300 nm to 380 nm is closely for the two types of films, but increasing largely in the longer wavelengths, especially from 380 nm to 410 nm, which is near to  $\text{TiO}_2$  band-gap edge wavelengths. In

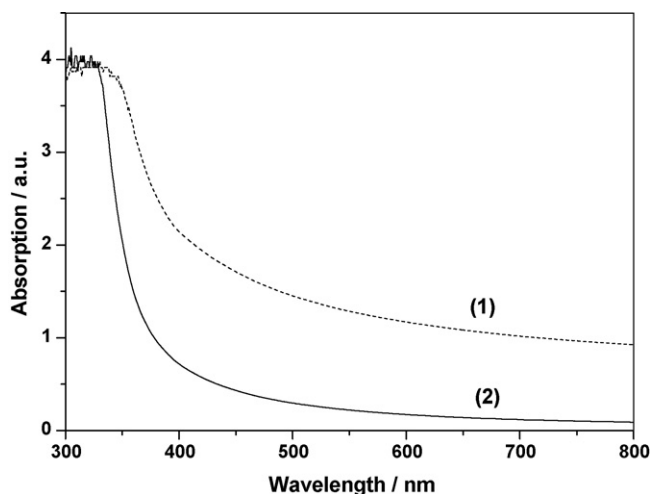


Fig. 5. (a) UV-vis absorption spectra of (1) TiO<sub>2</sub> micro-/nano-hierarchically porous film and (2) nano-structured film.

general, the onset of band-gap absorption of anatase TiO<sub>2</sub> is estimated 387 nm, which corresponds to 3.2 eV; the onset of band-gap absorption of rutile TiO<sub>2</sub> is 417 nm, which corresponds to 3.0 eV. The P25 TiO<sub>2</sub> material used here contains 78% anatase and 22% rutile, and the onset of its band-gap absorption is estimated 405–410 nm, which corresponding to ca. 3.08 eV. In the range of wavelength lower than 380 nm, UV light can be absorbed effectively by TiO<sub>2</sub> thin layer, thus there is no obvious enhanced light-collection effect from light scattering. But for the wavelengths from 380 nm to 410 nm, light scattering effect induced by hierarchical structure benefits for light collection. The enhanced photo-captured efficiency was also proved by the transmission spectra of the films (supporting information).

In addition, the BET specific surface area of porous films was confirmed by N<sub>2</sub> sorption analyses. The measured surface area of as-prepared nano-structured films is 53 g/m<sup>2</sup>. After introducing the hierarchical structure into the films, the specific surface area is improved to 67 g/m<sup>2</sup>. The increased surface area is due to intrusion of many macro-spheres, resulting in more inner TiO<sub>2</sub> nanoparticles exposed to the interface of gas/solid. Heterogeneous photocatalytic reaction often takes place in the interface of solid/liquid or solid/gas, so the surface condition of

catalysis is important. A large surface area can produce more active center of reaction to promote the reaction rate. It is the partial reason for the higher photocatalytic activity of hierarchical porous films.

Except for the contribution from increased light-collection efficiency and surface area, molecular transport is crucial for the mineralizing rate of pollutants. In the initial stage of photo-degradation, photogenerated holes in TiO<sub>2</sub> film are considered as important matters for oxidizing organic pollutants, possibly via a Russell-like mechanism [45,46]. The overall rate constant for photocatalytic reaction is composed of two factors, viz. the reaction on the surface and mass transfer of the pollutant toward the catalysts surface [42].

$$\frac{1}{K^*} = \frac{1}{K_m a_v} + \frac{1}{K_s k_{L-H}}$$

where  $K_s$  is the intrinsic surface reaction rate constant,  $k_{L-H}$  is the Langmuir–Hinshelwood adsorption constant,  $K_m$  is the mass diffusion coefficient, and  $a_v$  is the surface area of porous TiO<sub>2</sub> samples. In general, the rate of reaction between the hole and pollutants,  $K_s$ , is much quicker than the diffusion rate of the reactants to the active sites on the surface TiO<sub>2</sub> thin films [47–49]. Quite different from TiO<sub>2</sub> powder samples, the mass diffusion rate can be regarded as controlling step in the reaction of decomposing phenol when porous film servers as catalyst. So the suitable catalytic architectures will benefit for reactants, products and O<sub>2</sub> moving into and out of the catalytic system, and then achieve higher activity. It is interesting to be noted the magnification of increased activity for mineralization of liquid-phase phenol (60–70%) is bigger than that of gaseous CH<sub>3</sub>CHO (30–40%) with hierarchical structure. It may be explained as followed: for the gaseous molecules with high drift mobility, the diffusion of molecules in porous structure is easy and fast enough, thus the improvement of catalytic activity is limited with hierarchical structure. When liquid-phase phenol is selected, the diffusion action of species in porous structure will become the dominant and limiting step. The hierarchical structure gives unhampered channels for liquid-phase molecular transport, so the ratio of increased activity is larger than gaseous decomposition.

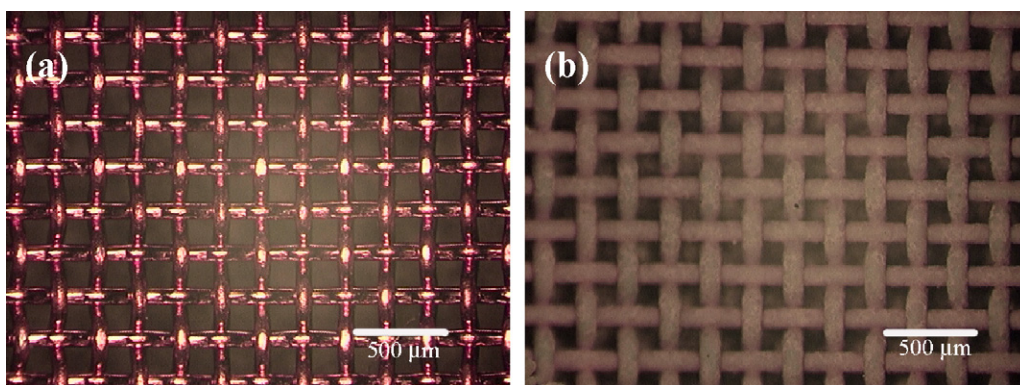


Fig. 6. Photograph of copper mesh (a) without and (b) with TiO<sub>2</sub> micro-/nano-hierarchically porous film.

As reported by Rolison [29], the transport of organic pollutant in media featuring large mesopores and macropores can approach rates of diffusion comparable to those in open medium. The beneficial effect of macro–nanoporosity on catalysis has been reported by Pinavania [30] and Yu [27]. To best of our knowledge, this is the first time to build up the hierarchical structure on the solid substrate with EHD technique and the enhanced photocatalytic activity for photocatalytic system is observed. Quite different from those powder materials, film photocatalyst is very important and promising for industrial application. Also the hierarchical thin films can be constructed continuously on any solid-state substrates in large-scale, such as copper mesh (Fig. 6), which give a broad actual application for air-cleaning and water decontamination.

#### 4. Conclusion

In summary, novel hierarchical porous TiO<sub>2</sub> films were introduced to conduct the photocatalytic researches and the catalytic mechanism was discussed here. The hierarchical porous films show the enhanced photocatalytic activity comparing to those of nano-structured films, and they suit for mineralizing pollutants of different phases. This is the first time to fabricate the hierarchical porous structure in film photocatalysis by EHD technique, and also the large-area preparation of the high-efficiency film photocatalysis will provide an attractive opportunity to industrial application.

#### Acknowledgments

This work was supported by a Grant-in-Aid for Scientific Research on Priority Area 417 and the Asia S&T Strategic Cooperation Program from the Japanese Ministry of Education, Culture, Sports, Science and Technology, the National Natural Science Foundation of China (20573120, 50533030), the National Research Fund for Fundamental Key Projects (2006CB806200, 2006CB932100 and 2007CB936403). Hide-nori Saito is greatly thanked for conducting the SEM measurements. We would like to thank Drs. Xiao Chen and Zhongjun Cheng of Institute of Chemistry, Chinese Academy of Sciences for their helpful discussions.

#### Appendix A. Supplementary data

Supplementary data associated with this article can be found, in the online version, at doi:10.1016/j.apcatb.2008.01.035

#### References

- [1] A. Fujishima, K. Honda, *Nature* 238 (1972) 37.
- [2] C.K. Xu, R. Killmeyer, M.L. Gray, S.U.M. Khan, *Electrochem. Commun.* 8 (2006) 1650.
- [3] J. Nowotny, T. Bak, M.K. Nowotny, L.R. Sheppard, *J. Phys. Chem. B* 110 (2006) 18492.
- [4] J.H. Park, S. Kim, A.J. Bard, *Nano Lett.* 6 (2006) 24.
- [5] B. O'Regan, M. Grätzel, *Nature* 353 (1991) 737.
- [6] S. Nishimura, N. Abrams, B.A. Lewis, L.I. Halaoui, T.E. Mallouk, K.D. Benkstein, J. van de Lagemaat, A.J. Frank, *J. Am. Chem. Soc.* 125 (2003) 6306.
- [7] R. Wang, K. Hashimoto, A. Fujishima, M. Chikuni, E. Kojima, A. Kitamura, M. Shimohigoshi, T. Watanabe, *Nature* 388 (1997) 431.
- [8] M. Miyauchi, A. Nakajima, K. Hashimoto, T. Watanabe, *Adv. Mater.* 12 (2000) 1923.
- [9] S.A. O'Neill, R.J.H. Clark, I.P. Parkin, N. Elliott, A. Mills, *Chem. Mater.* 15 (2003) 46.
- [10] M.R. Hoffmann, S.T. Martin, W. Choi, D.W. Bahnemann, *Chem. Rev.* 95 (1995) 69.
- [11] R. Asahi, T. Morikawa, T. Ohwaki, K. Aoki, Y. Taga, *Science* 293 (2001) 269.
- [12] Y.H. Ng, S. Ikeda, T. Harada, S. Higashida, T. Sakata, H. Mori, M. Matsumura, *Adv. Mater.* 19 (2007) 597.
- [13] A.M. Peiro, G. Doyle, A. Mills, J.R. Durrant, *Adv. Mater.* 17 (2005) 2365.
- [14] Y.B. Mao, S.S. Wong, *J. Am. Chem. Soc.* 128 (2006) 8217.
- [15] J. Yang, C.C. Chen, H.W. Ji, W.H. Ma, J.C. Zhao, *J. Phys. Chem. B* 109 (2005) 21900.
- [16] J. Joo, S.G. Kwon, T. Yu, M. Cho, J. Lee, J. Yoon, T. Hyeon, *J. Phys. Chem. B* 109 (2005) 15297.
- [17] J.M. Wu, *Environ. Sci. Technol.* 41 (2007) 1723.
- [18] V. Subramanian, E.E. Wolf, P.V. Kamat, *J. Am. Chem. Soc.* 126 (2004) 4943.
- [19] D. Lahiri, V. Subramanian, B.A. Bunker, P.V. Kamat, *J. Chem. Phys.* 124 (2006) 204720.
- [20] X.W. Zhang, M.H. Zhou, L.C. Lei, *Catal. Commun.* 7 (2006) 427.
- [21] G. Colon, M. Maicu, M.C. Hidalgo, J.A. Navio, *Appl. Catal. B-Environ.* 67 (2006) 41.
- [22] S. Livraghi, M.C. Paganini, E. Giamello, A. Selloni, C. Di Valentin, G. Pacchioni, *J. Am. Chem. Soc.* 128 (2006) 15666.
- [23] R.S. Dibble, G.R. Soja, R.M. Hoth, D.F. Watson, *Langmuir* 23 (2007) 3432.
- [24] J.H. Pan, W.I. Lee, *Chem. Mater.* 18 (2006) 847.
- [25] H. Kim, W. Choi, *Appl. Catal. B-Environ.* 69 (2007) 127.
- [26] V.N. Kuznetsov, N. Serpone, *J. Phys. Chem. B* 110 (2006) 25203.
- [27] L.Z. Zhang, J.C. Yu, *Chem. Commun.* (2003) 2078.
- [28] H. Choi, A.C. Sofranko, D.D. Dionysiou, *Adv. Funct. Mater.* 16 (2006) 1067.
- [29] D.R. Rolison, *Science* 299 (2003) 1698.
- [30] P.T. Tanev, T.J. Pinnavaia, *Science* 271 (1996) 1267.
- [31] T.R. Pauly, Y. Liu, T.J. Pinnavaia, S.J.L. Billinge, T.P. Rieker, *J. Am. Chem. Soc.* 121 (1999) 8835.
- [32] M. Jin, X. Zhang, A.V. Emeline, Z. Liu, D.A. Tryk, T. Murakami, A. Fujishima, *Chem. Commun.* (2006) 4483.
- [33] C.R. Xiong, K.J. Balkus, *Chem. Mater.* 17 (2005) 5136.
- [34] H.G. Yu, J.G. Yu, B. Cheng, S.W. Liu, *Nanotechnology* 18 (2007) 065604.
- [35] X. Quan, S.G. Yang, X.L. Ruan, H.M. Zhao, *Environ. Sci. Technol.* 39 (2005) 3770.
- [36] A. Yamamoto, H. Imai, *J. Catal.* 226 (2004) 462.
- [37] X.Z. Li, H. Liu, *Environ. Sci. Technol.* 37 (2003) 3989.
- [38] Y.Z. Li, T. Kunitake, S. Fujikawa, *J. Phys. Chem. B* 110 (2006) 13000.
- [39] S.H. Baeck, K.S. Choi, T.F. Jaramillo, G.D. Stucky, E.W. McFarland, *Adv. Mater.* 15 (2003) 1269.
- [40] W.K. Ho, J.C. Yu, J.G. Yu, *Langmuir* 21 (2005) 3486.
- [41] Y. Zhao, J. Zhai, S.X. Tan, L.F. Wang, L. Jiang, D.B. Zhu, *Nanotechnology* 17 (2006) 2090.
- [42] M.M. Ren, R. Ravikrishna, K.T. Valsaraj, *Environ. Sci. Technol.* 40 (2006) 7029.
- [43] A. Fujishima, T.N. Rao, D.A. Tryk, *J. Photochem. Photobiol. C-Photochem. Rev.* 1 (2000) 1.
- [44] A. Heller, *Acc. Chem. Res.* 28 (1995) 503.
- [45] J. Schwitzgebel, J.G. Ekerdt, H. Gerischer, A. Heller, *J. Phys. Chem. B* 99 (1995) 5633.
- [46] Y. Cao, X.T. Zhang, W.S. Yang, H. Du, Y.B. Bai, T.J. Li, J.N. Yao, *Chem. Mater.* 12 (2000) 3445.
- [47] D.L. Jiang, S.Q. Zhang, H.J. Zhao, *Environ. Sci. Technol.* 41 (2007) 303.
- [48] K.J. Buechler, R.D. Noble, C.A. Koval, W.A. Jacoby, *Ind. Eng. Chem. Res.* 38 (1999) 892.
- [49] S.P. Albu, A. Ghicov, J.M. Macak, R. Hahn, P. Schmuki, *Nano Lett.* 7 (2007) 1286.